AN OVERVIEW OF USING KINEMATIC REDUNDANCY TO CREATE FAILURE TOLERANT ROBOTS

A. A. MACIEJEWSKI, V. BALAKRISHNAN, J. D. ENGLISH,
M. GOEL, K. N. GROOM, C. L. LEWIS, R. G. ROBERTS

Purdue University
1285 Electrical Engineering Building
West Lafayette, Indiana 47907-1285
maciejew@ecn.purdue.edu

Abstract. Kinematically redundant manipulators have been proposed for use in critical applications due to their ability to compensate for failures in individual joints. This article presents an overview of the current state of the art in utilizing kinematic redundancy to instill failure tolerance into robotic systems. Techniques are presented for improving performance prior to failures, anticipating impending errors in order to minimize their impact, and guaranteeing a specified level of performance after failures. These techniques are illustrated for both a locked-joint failure model and a free-swinging joint failure model, which together account for a large fraction of typical joint failure modes.

Key Words. robot; manipulator; kinematically redundant; redundant robot; fault/failure tolerance.

1. INTRODUCTION

Failures in robotic systems are not an uncommon occurrence [8]. A report from the Japanese Ministry of Labor indicates that over 60% of the industrial robots studied had a mean-time-between-failure of less than 500 hours; indeed, 28.7% had mean-time-between-failure of 100 hours or less [6]. These failures have significant consequences, ranging from economic impact in industrial applications to potentially catastrophic incidents in remote and/or hazardous environments [5]. A direct approach towards increasing robot reliability is to improve the reliability of the individual components [26]; however, achieving acceptable reliability rates is often prohibitively expensive, and sometimes technologically impossible. An alternate approach is to consider failure-tolerant robot designs. These typically incorporate a failure detection and identification scheme [30, 31] followed by failure recovery [29]. Designing the robot with redundant systems increases the options available for failure tolerance. Redundancy can be in the form of duplication of actuators and sensors [28, 32], or in the form of kinematic redundancy [16, 19, 21, 23], which is the topic of this work.

It is well known that the kinematic structure of a redundant manipulator must be carefully designed to guarantee that the additional degrees of freedom support failure tolerance [19]. Ideally, kinematic redundancy will provide greater dexterity prior to failures, minimize the immediate impact of a failure, and guarantee task completion by ensuring a reachable post-failure workspace. All of these desirable characteristics require that one consider both local dexterity measures, typically centered around the manipulator Jacobian [10, 11, 13, 16, 20, 24, 25], as well as global measures such as the post-failure workspace [9, 12, 17, 22]. Many times these measures can be related, for example, workspace boundaries re-

sult in manipulator singularities that are easily identified by examining the Jacobian. This paper presents an overview of our work in both of these areas for two different types of failure modes, i.e., locked joint failures and free-swinging joint failures.

2. LOCAL FAULT TOLERANCE

2.1. Background

The position[1] of the end effector of a manipulator can be expressed in terms of its joint variables by the kinematic equation

$$\mathbf{x} = f(\mathbf{q}), \tag{1}$$

where $\mathbf{x} \in I\!R^m$ is the position of the end effector, $\mathbf{q} \in I\!R^n$ is the vector of joint variables, and m and n the dimensions of the task space and joint space respectively. Redundant manipulators, by definition, have more degrees of freedom (DOFs) than required for a task, i.e., $n > m$, where $n - m$ is the degree of redundancy. The end-effector velocity $\dot{\mathbf{x}}$ is expressed in terms of the joint rates $\dot{\mathbf{q}}$ as

$$\dot{\mathbf{x}} = J\dot{\mathbf{q}}, \tag{2}$$

where $J \in I\!R^{m\times n}$ is the manipulator Jacobian. For redundant manipulators, (2) is underconstrained and there are an infinite number of solutions which can be expressed as

$$\dot{\mathbf{q}} = J^+\dot{\mathbf{x}} + \left(I - J^+J\right)\mathbf{z}, \tag{3}$$

where J^+ is the pseudoinverse of the Jacobian, and $\mathbf{z} \in I\!R^n$. The first term on the right in (3) corresponds to the least-squares minimum-norm solution, while the second is the projection of the vector $\mathbf{z}$ onto the null space of the Jacobian. The vector $\mathbf{z}$ is frequently chosen as $\mathbf{z} = \nabla h(\mathbf{q})$ in order to optimize some desirable secondary criterion given by h, under exact end-effector tracking [18]. Other methods for optimizing h, such as those based on the extended Jacobian [3] or the augmented Jacobian [7, 27], also require its gradient.

The Singular Value Decomposition (SVD) provides a mathematical framework for describing both the optimization scheme (3), as well as many of the failure-tolerance measure considered here. The SVD of the Jacobian is the matrix factorization

$$J = U\Sigma V^T \tag{4}$$

where $U \in I\!R^{m\times m}$ is an orthogonal matrix of the left singular vectors $\hat{\mathbf{u}}_i$, and $V \in I\!R^{n\times n}$ is an orthogonal matrix of the right singular vectors $\hat{\mathbf{v}}_i$. The matrix Σ is m by n, with $\Sigma = [\Sigma_d\ \mathbf{0}]$, where $\Sigma_d = \mathrm{diag}(\sigma_1, \ldots, \sigma_m)$ and $\mathbf{0}$ is an m by $n - m$ zero matrix. The σ_i are called the singular values of J, and satisfy $\sigma_1 \geq \sigma_2 \geq \cdots \geq \sigma_m \geq 0$. The rank r of J is simply the number of its nonzero singular values.

The SVD has long been a valuable tool for quantifying various dexterity measures: manipulability [33] (product of the singular values), isotropy [1, 15] (ratio of the maximum singular value to the minimum), task compatibility [4] (weighted combination of singular values) and proximity to singularities [14] (minimum singular value). Each of these measures has its own physical interpretation and can be used for quantifying the capabilities of a manipulator both before or after a failure.

2.2. Locked Joint Failures

The effect of a single locked joint failure of joint i is easily incorporated into the manipulator Jacobian by simply removing the ith column, i.e.,

$${}^iJ_{m\times n-1} = \left[\ \mathbf{j}_1\ \ \mathbf{j}_2\ \ \cdots\ \ \mathbf{j}_{i-1}\ \ \mathbf{j}_{i+1}\ \ \cdots\ \ \mathbf{j}_n\ \right], \tag{5}$$

or equivalently, replacing the ith column with zeros. One can then apply any of the local dexterity measures discussed above to the resulting post-failure Jacobian, ${}^iJ$, to determine the manipulator's local tolerance to a failure in joint i. The two most commonly applied local measures of fault tolerance are the reduction in manipulability [25] (due to ease of analysis), and the minimum singular value [13, 16, 19, 20] (a worst-case measure). As an example of a worst-case measure, consider the following kinematic fault-tolerance measure:

$$\mathcal{K} = \min_{i=1\ldots n} \sigma_m\left({}^iJ\right). \tag{6}$$

This measure can be re-expressed in terms of the singular vectors of the failed Jacobian ${}^FJ$ (where F denotes the index of the most debilitating joint failure) as

$$\mathcal{K} = {}^F\hat{\mathbf{u}}_m^T\ {}^FJ\ {}^F\hat{\mathbf{v}}_m. \tag{7}$$

The change of $\mathcal{K}$ with respect to q_i is then given by

$$\frac{\partial \mathcal{K}}{\partial q_i} = {}^F\hat{\mathbf{u}}_m^T\ \frac{\partial\ {}^FJ}{\partial q_i}\ {}^F\hat{\mathbf{v}}_m. \tag{8}$$

which can be used in the gradient[2] projection scheme suggested by (3), thereby maximizing the manipulator's failure tolerance while exactly tracking $\dot{\mathbf{x}}$. An algorithm for performing these computations in real time is given in [13].

[1] The term "position" is used to refer to any combination of position and/or orientation variables.

[2] Note that $\mathcal{K}$ is not differentiable when F is not unique. However, this can be addressed through standard numerical techniques.

The above control scheme guarantees that the current configuration of the manipulator will be optimal in the sense that it maximizes $\mathcal{K}$ for the desired end-effector position. However, it is instructive to consider the extremal values of $\mathcal{K}$ over all possible manipulator designs and configurations. If one constrains the configurations to those that are isotropic [1, 14, 15] prior to failure, then it is easy to show that for single joint failures

$$0 \leq \mathcal{K} \leq \sigma \sqrt{\frac{n-m}{n}} \tag{9}$$

where σ denotes the norm of the pre-failure Jacobian [20]. Furthermore, it is possible to determine a canonical form for Jacobians that achieve the maximal value of $\mathcal{K}$. For example, for a four DOF manipulator required to position in three-dimensional space, an optimally failure tolerant Jacobian is given by

$$J = \begin{bmatrix} -\sqrt{\frac{3}{4}} & \sqrt{\frac{1}{12}} & \sqrt{\frac{1}{12}} & \sqrt{\frac{1}{12}} \\ 0 & -\sqrt{\frac{2}{3}} & \sqrt{\frac{1}{6}} & \sqrt{\frac{1}{6}} \\ 0 & 0 & -\sqrt{\frac{1}{2}} & \sqrt{\frac{1}{2}} \end{bmatrix}. \tag{10}$$

Note that the null vector of J in this case is given by $\begin{bmatrix} 1 & 1 & 1 & 1 \end{bmatrix}^T$, i.e., all elements are of equal magnitude, which is a characteristic of optimally failure tolerant Jacobians. At the other end of the spectrum, it is also easy to show that $\mathcal{K} = 0$ whenever the ith element of the null vector of J is equal to zero, which corresponds to a rank deficient post-failure Jacobian, ${}^iJ$. These results are similar to those obtained when using the manipulability-based failure tolerance measure, with analogous results for multiple joint failures [25].

2.3. Free-Swinging Joint Failures

This section considers a local measure of fault tolerance with respect to free-swinging type joint failures. A free-swinging failure is defined as a failure that prevents the application of actuator torque on a manipulator's joint so that the failed joint moves under the influence of external forces and gravity. While there are many measures that have been proposed for quantifying failure tolerance to free-swinging failures [10], [11], this section will use the swing angle as an illustrative example. The swing angle $\hat{\theta}_i$ is defined as the angle through which a failed rotational joint i moves after a failure, that is, the angle between the prefailure configuration and the settled, post-failure configuration. The resting position is that for which the center of mass of the portion of the manipulator outboard from the failed joint is at its lowest position relative to the gravitational field. The expectation is that with a small swing angle, the manipulator is less likely to cause secondary damage to itself or its environment. A shortcoming of a swing-angle based measure is that it provides a limited amount of information on the Cartesian motion of the manipulator [10].

The value of $\hat{\theta}_i$ depends on several geometric parameters. Let $\hat{z}_\ell$ denote the unit vector along joint $\ell+1$, the z-axis of the ℓ^{th} Denavit-Hartenberg (D-H) coordinate frame; $\vec{s}^*_\ell$ denote the first moment of inertia of the composite rigid body formed by links $\ell+1$ through n referred to the origin of D-H frame ℓ; and $\vec{g}$ denote the gravity vector in the upward direction. The angle through which joint i would swing were it to fail is given by the angle between the projections of $\vec{s}^*_{i-1}$ and $-\vec{g}$ onto the plane perpendicular to $\hat{z}_{i-1}$ (the axis of rotation). This can be calculated as the angle between $(\vec{s}^*_{i-1} \times \hat{z}_{i-1})$ and $(\hat{z}_{i-1} \times \vec{g})$, i.e.,

$$\cos(\hat{\theta}_i) = \frac{(\vec{s}^*_{i-1} \times \hat{z}_{i-1}) \cdot (\hat{z}_{i-1} \times \vec{g})}{\|\vec{s}^*_{i-1} \times \hat{z}_{i-1}\| \, \|\hat{z}_{i-1} \times \vec{g}\|}; \tag{11}$$

$$\sin(\hat{\theta}_i) = \frac{\hat{z}_{i-1} \cdot (\vec{g} \times \vec{s}^*_{i-1})}{\|\vec{s}^*_{i-1} \times \hat{z}_{i-1}\| \, \|\hat{z}_{i-1} \times \vec{g}\|}. \tag{12}$$

Provided neither $\vec{s}^*_{i-1}$ nor $\vec{g}$ is parallel to $\hat{z}_{i-1}$, equations (11) and (12) give

$$\hat{\theta}_i = \text{Atan2}[\hat{z}_{i-1} \cdot (\vec{g} \times \vec{s}^*_{i-1}), (\vec{s}^*_{i-1} \times \hat{z}_{i-1}) \cdot (\hat{z}_{i-1} \times \vec{g})], \tag{13}$$

where the range of Atan2 is $-\pi$ to π; otherwise the torque on joint i is zero and $\hat{\theta}_i = 0$. The value $\hat{\theta}_i$ represents the failure-susceptibility measure of joint i alone. For an n DOF manipulator, a column of joint measures is given by $\hat{\theta} = \begin{bmatrix} \hat{\theta}_1 & \hat{\theta}_2 & \cdots & \hat{\theta}_n \end{bmatrix}^T$. For positive semidefinite weighting matrix W, the form of a comprehensive failure-susceptibility measure $h(\mathbf{q})$ is given by

$$h(\mathbf{q}) = \hat{\theta}^T(\mathbf{q}) W \hat{\theta}(\mathbf{q}). \tag{14}$$

As with the local optimization of $\mathcal{K}$ in the previous section, the gradient [11] of $h(\mathbf{q})$ can be used in (3) to minimize the effects of a potential free-swinging joint failure while performing the desired task.

3. FAULT TOLERANT WORKSPACE

3.1. Locked Joint Failures

The post-failure workspace of a kinematically redundant manipulator is closely related to the null space of the manipulator Jacobian [17, 24]. The null space defines the tangent hyperplane to the self-motion manifold, whose size and shape can be used as a measure of fault tolerance. As a simple example, consider the three DOF planar manipulator shown in Fig. 1, where a projection of its

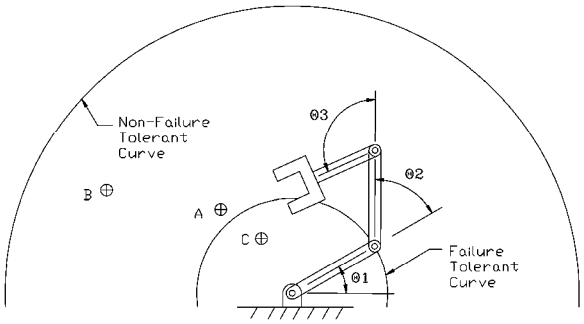

Fig. 1: A three DOF planar manipulator with equal link lengths is shown with the curves in the workspace having maximum and minimum failure tolerance capabilities. The points A, B, and C are representative task space points that are analyzed for their global failure tolerance properties.

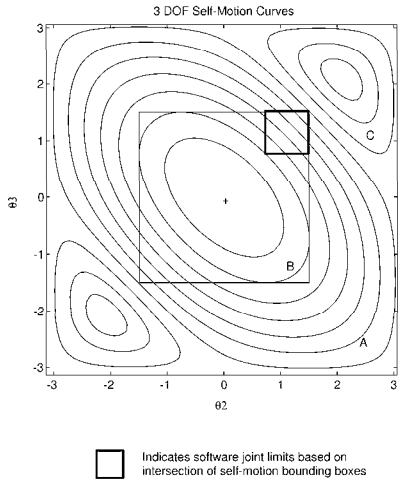

Fig. 2: The set of joint configurations that keep the manipulator's end-effector at a single 2D position form curves in the configuration space of the manipulator. The curves shown are the self-motion curves for the 3 link planar manipulator depicted in Fig. 1. The self-motion curves for some regions of the workspace are markedly larger than others. Points with large self-motion curves tend to be more failure tolerant.

self-motion curves onto the (θ_2,θ_3) plane is shown in Fig. 2. Each curve represents the set of joint configurations that place the end-effector at a constant radius from the base. From the figure, one can see that some regions of the workspace have larger self-motion manifolds than others. For instance, the points at the boundary of the workspace are reachable in only a single joint configuration, which corresponds to the self-motion manifold also being a point. Clearly, workspace boundary points are unlikely to be reachable after any joint failure. In contrast, the workspace points at exactly one link length from the base have self-motion manifolds which span the entire range of joint values for all three joints. In this unique case the failed manipulator will always be able to reach the entire set of points one link length from the base regardless of which joint fails, or the configuration in which it fails.

To guarantee that a manipulator is capable of returning to a critical workspace position, the motion range for each of the n joints must be constrained to lie within the range spanned by the self-motion manifold associated with that position. This effectively superscribes an n-dimensional bounding box aligned with the joint axes around the self-motion manifold.[3] The size of the self-motion manifold bounding box is a measure of the inherent failure tolerance of its associated workspace position. If the manipulator fails while operating within the bounding box of a given desired end-effector position x^*, then it will always be able to position its end-effector at x^* regardless of where the end-effector is when the failure occurs.

As a specific example, consider again the 3 DOF manipulator for which the bounding boxes associated with the self-motion surfaces for the three workspace points labeled A, B, and C in Fig. 1 have been drawn in Fig. 2. Note that although θ_1 and its associated boundaries are not shown, they also need to be considered. If we want to guarantee that task point A is reachable after any single joint failure, the joint values must be restricted to the range of the bounding box for A's associated self-motion manifold. Now, if in addition we want to guarantee that task point B is reachable after any single joint failure, the joint values must be further restricted to B's bounding box (which is the intersection of boxes A and B). Notice that if the manipulator is in a configuration near the center of bounding box B when a joint failure occurs, then the artificial joint restrictions must be released for the manipulator to reach task point A. Finally, consider trying to add task point C to this scenario. The intersection of the three bounding boxes is indicated with a bold line in Fig. 2. By design if a joint fails while operating in this region then by relaxing these artificial joint limits, the manipulator can reach all three task points, however, with these artificial joint restrictions in place, task point C is unreachable.

Thus constraining the motion of a manipulator's joints prior to a failure will, in general, render a significant portion of the original workspace unreachable. However, imposing appropriate software joint limits prior to a failure is crucial for increasing the size of the workspace that can be guaranteed reachable after an arbitrary failure.

[3]Note that the values for the bounding box are easily calculated by identifying zero elements in the null vector which also correspond to $\mathcal{K} = 0$.

3.2. Undetected Locked Joint Failures

All of the above work assumes that the failure of a joint is identified by the controller so that it can modify it's commands to the remaining functional joints. While this is a reasonable assumption for many cases, there are situations where this may not be possible. It is interesting to note that the reachability of a desired task position, i.e., whether it lies in the post-failure workspace, is the dominant factor in whether the manipulator will eventually be able to complete its task, even if a joint failure is not recognized. In addition, the conditions under which a manipulator will not achieve the desired task position are closely related to the minimal values of the local failure tolerance measures discussed above. This is formally presented in the following theorem [12].

Theorem 1 Consider a manipulator at a non-singular configuration, driven by a generalized inverse control

$$\dot{\mathbf{q}}_c = G\dot{\mathbf{x}}_c, \tag{15}$$

where $G = W^{-1}J^T(JW^{-1}J^T)^{-1}$ for some symmetric $W > 0$. Let S be the set of the indices of the k locked joints, $\mathbf{j}_i$ denote the i-th column of J, and $\mathbf{e}_i$ denote the i-th natural basis vector. Then,

1. Only the failed joints are commanded motion if and only if the commanded end-effector velocity vector $\dot{\mathbf{x}}_c$ lies in the space spanned by the columns corresponding to the failed joints of the Jacobian, i.e.,

$$\dot{\mathbf{q}}_c = \sum_{i\in S} \alpha_i \mathbf{e}_i \Longleftrightarrow \dot{\mathbf{x}}_c = \sum_{i\in S} \alpha_i \mathbf{j}_i, \tag{16}$$

   for some $\alpha_i \in I\!R$, $i \in S$

2. Moreover, the failed joints are commanded non-zero velocities only if a post-failure weighted Jacobian is rank deficient, i.e.,

$$\dot{\mathbf{q}}_c = \sum_{i\in S} \alpha_i \mathbf{e}_i \neq \mathbf{0} \Longrightarrow {}^i(JW^{-1}) \text{ rank deficient}, \tag{17}$$

   where ${}^i(JW^{-1}) \in I\!R^{m\times(n-k)}$ is obtained from JW^{-1} by zeroing the columns with indices $i \in S$.

Kinematic redundancy can be used to guarantee the post-failure reachability of task positions as discussed above, however, if a locked-joint failure is not detected, then the manipulator may or may not eventually reached the desired position. For example, consider a planar 3-DOF manipulator under pseudoinverse control that is required to move from an initial position $\mathbf{x}_i$ to a desired task position $\mathbf{x}_d$. In Fig. 3, the manipulator is able to successfully complete the task even with an undetected failure of joint 2. Illustrated in Fig. 4 is a case of erroneous convergence, where, even though the desired task position $\mathbf{x}_d$ is the same as in Fig. 3 (and lies in the post-failure workspace after a failure of joint 1), the manipulator converges elsewhere. These different convergence behaviors are characterized by the properties of the configurations to which a manipulator erroneously converges as outlined in the above theorem.

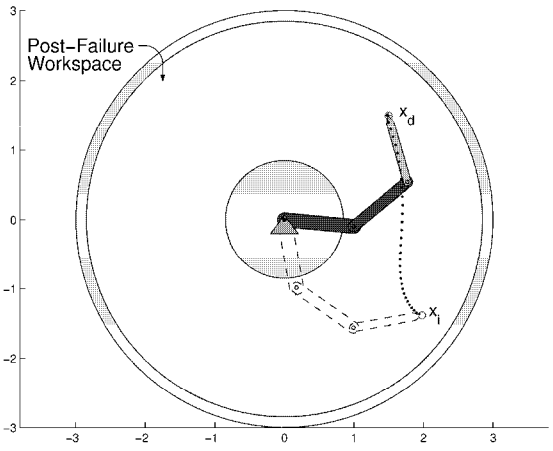

Fig. 3: Successful convergence to the task position. The manipulator is able to complete the point-to-point motion task between $\mathbf{x}_i$ and $\mathbf{x}_d$, even with a failure of joint 2. ($\mathbf{x}_i = [2.0\ -1.4]^T$ and $\mathbf{x}_d = [1.5\ 1.5]^T$).

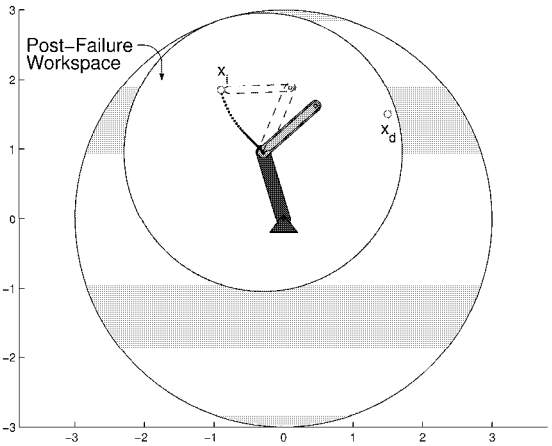

Fig. 4: Erroneous convergence when the desired task position $\mathbf{x}_d$ is in the post-failure workspace. With a joint 1 failure the manipulator converges to a configuration where the "reduced-manipulator" becomes singular (${}^1J = [\mathbf{j}_2\ \mathbf{j}_3]$ rank deficient), and $\dot{\mathbf{x}}_c$ and $\mathbf{j}_1$ align. ($\mathbf{x}_i = [-0.9\ 1.8]^T$ and $\mathbf{x}_d = [1.5\ 1.5]^T$).

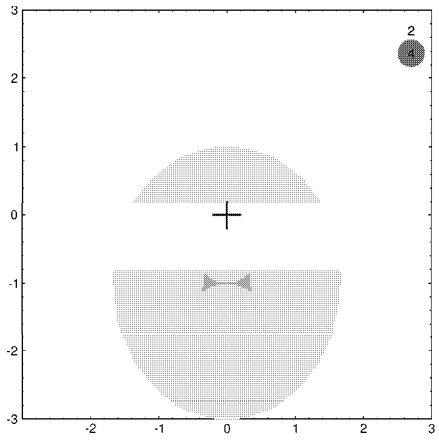

Fig. 5: The boundaries of the post-failure workspace and the number of solutions within each boundary for a 3 DOF, unity link length and mass, example manipulator following a failure of joint two. Any point in the light-gray region can be reached with two distinct configurations after a failure of the second joint, and each point in the dark-gray region can be reached with four.

3.3. Free-Swinging Joint Failures

After a free-swinging failure, the failed joint moves under the influence of external forces and gravity. This motion results in the potential for secondary damage due to collisions with the environment. Techniques for minimizing this motion were discussed in section 2.3. and in [10, 11]. However, this motion also presents the possibility of expanded usefulness after a failure [2]. It is the issue of usefulness after a failure, in terms of the post-failure workspace, that is the topic of this section. The post-failure workspace is defined here as the set of all hand poses reachable by the manipulator when stationary with zero actuator torque on the failed joint (essentially equivalent to the zero swing angle case discussed in section 2.3.). By differentiating the constraints for maintaining zero torque on a joint and tracking the rank deficiency of the corresponding augmented Jacobian [9], one can efficiently trace the post-failure workspace boundary for any general manipulator.

The results of this technique are illustrated on a simple three DOF manipulator with link lengths of unity, link masses of unity, and link centers of mass at the link centers. The results for a failure of joint two are shown in Fig. 5. The regions shown are for stable solutions, meaning the center of mass of the portion of the manipulator outboard from the failed joint lies below the failed joint applies). Any workspace point corresponding to a stable solution can be reached after a failure simply by moving the healthy joints to their required positions along an arbitrary path. The number of solutions within a given boundary are obtained by selecting any location within the region and determining the number of zero-torque configurations that correspond to that location. Four configurations reaching a point within the dark gray region of Fig. 5 are shown in Fig. 6. For all the configurations, the composite center of mass of links two and three lies directly below the second joint.

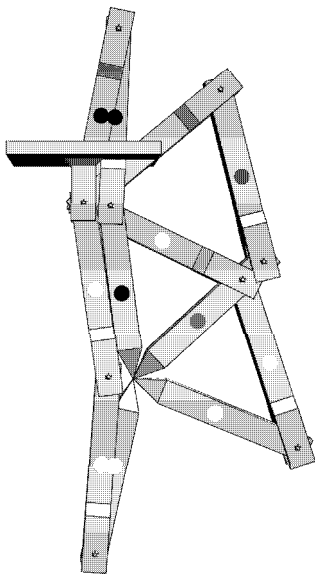

Fig. 6: Four configurations reaching the point $(.41, -1.01)$ with no torque on joint two. This point lies within the dark-gray region of Fig. 5. For each configuration, the center of mass of the composite body formed by links two and three lies below joint two, making each configuration stable.

4. CONCLUSIONS

The main conclusion of the work presented here is that kinematic redundancy can be very effective for providing a prescribed degree of tolerance to joint failures. However, the degree of failure tolerance is strongly dependent on the kinematic design of the manipulator and on the manner in which redundancy resolution is performed prior to a failure. Redundancy that is improperly incorporated and/or utilized can be rendered useless.

5. ACKNOWLEDGEMENTS

This work was supported by Sandia National Laboratories under contract numbers 18-4379B and AL-3011. Additional support was provided by the National Science Foundation under grant CDR 8803017 to the Engineering Research Center for Intelligent Manufacturing Systems, a NASA graduate student research fellowship (grant number NGT9-2) and by the National Research Council.

References

[1] J. Angeles. The design of isotropic manipulator architectures in the presence of redundancies. *Int. J. Robotics Res.*, 11(3):196–201, June 1992.

[2] H. Arai and S. Tachi. Position control of a manipulator with passive joints using dynamic coupling. *IEEE Trans. Robotics and Automation*, 7(4):528–534, 1991.

[3] J. Baillieul. Kinematic programming alternatives for redundant manipulators. *IEEE Int. Conf. Robotics and Automation*, pp. 722–728, St. Louis, MO, Mar. 25-28, 1985.

[4] S. L. Chiu. Task compatibility of manipulator postures. *Int. J. Robotics Res.*, 7(5):13–21, Oct. 1988.

[5] R. Colbaugh and M. Jamshidi. Robot manipulator control for hazardous waste-handling applications. *J. Robotic Systems*, 9(2):215–250, 1992.

[6] B. S. Dhillon. *Robot Reliability and Safety.* Springer-Verlag, New York, 1991.

[7] O. Egeland. Task-space tracking with redundant manipulators. *IEEE J. Robotics and Automation*, RA-3(5):471–475, Oct. 1987.

[8] J. F. Engelberger. Three million hours of robot field experience. *Industrial Robot*, pp. 164-168, June 1974.

[9] J. D. English and A. A. Maciejewski. Robotic workspaces after a free-swinging failure. *J. of Intelligent and Robotic Systems*, 19(1):55–72, May 1996.

[10] J. D. English and A. A. Maciejewski. Euclidean-space measures of robotic joint failures. *IEEE Int. Conf. Robotics and Automation*, pp. 2894–2901, Albuquerque, NM, Apr. 20-25, 1997.

[11] J. D. English and A. A. Maciejewski. Fault tolerance for kinematically redundant manipulators: Anticipating free-swinging joint failures. Accepted to appear in *IEEE Trans. Robotics and Automation.*

[12] M. Goel, A. A. Maciejewski, and V. Balakrishnan. An analysis of the post-fault behavior of robotic manipulators. *IEEE Int. Conf. Robotics and Automation*, pp. 2583–2588, Albuquerque, NM, Apr. 20-25, 1997.

[13] K. N. Groom, A. A. Maciejewski, and V. Balakrishnan. Real-time failure tolerant control of kinematically redundant manipulators. *IEEE Int. Conf. Robotics and Automation*, pp. 2595–2600, Albuquerque, NM, Apr. 20-25, 1997.

[14] C. A. Klein and B. E. Blaho. Dexterity measures for the design and control of kinematically redundant manipulators. *Int. J. Robotics Res.*, 6(2):72–83, Summer 1987.

[15] C. A. Klein and T. Miklos. Spatial robotic isotropy. *Int. J. Robotics Res.*, 10(4):426–437, Aug. 1991.

[16] C. L. Lewis and A. A. Maciejewski. Dexterity optimization of kinematically redundant manipulators in the presence of failures. *Computers and Electrical Eng.*, 20(3):273–288, May 1994.

[17] C. L. Lewis and A. A. Maciejewski. Fault tolerant operation of kinematically redundant manipulators for locked joint failures. *IEEE Trans. Robotics and Automation*, 13(4):622–629, Aug. 1997.

[18] A. Liégeois. Automatic supervisory control of the configuration and behavior of multibody mechanisms. *IEEE Trans. Systems, Man, and Cybernetics*, SMC-7(12):868–871, Dec. 1977.

[19] A. A. Maciejewski. Fault tolerant properties of kinematically redundant manipulators. *IEEE Int. Conf. Robotics and Automation*, pp. 638–642, Cincinnati, OH, May 13-18, 1990.

[20] A. A. Maciejewski and R. G. Roberts. On the existence of an optimally failure tolerant 7R manipulator Jacobian. *Applied Mathematics and Computer Science*, 5(2):343–357, 1995.

[21] C. J. J. Paredis, W. K. F. Au, and P. K. Khosla. Kinematic design of fault tolerant manipulators. *Computers and Electrical Eng.*, 20(3):211–220, May 1994.

[22] C. J. J. Paredis and P. K. Khosla. Mapping tasks into fault tolerant manipulators. *IEEE Int. Conf. Robotics and Automation*, pp. 696–703, San Diego, CA, May 8-13, 1994.

[23] A. K. Pradeep, P. J. Yoder, R. Mukundan, and R. J. Schilling. Crippled motion in robots. *IEEE Trans. Aerospace Electronic Systems*, 24(1):2–13, Jan. 1988.

[24] R. G. Roberts. On the local fault tolerance of a kinematically redundant manipulator. *J. Robotic Systems*, 13(10):649–661, 1996.

[25] R. G. Roberts and A. A. Maciejewski. A local measure of fault tolerance for kinematically redundant manipulators. *IEEE Trans. Robotics and Automation*, 12(4):543–553, Aug. 1996.

[26] D. L. Schneider, D. Tesar, and J. W. Barnes. Development & testing of a reliability performance index for modular robotic systems. *Proc. Annual Reliability and Maintainability Symp.*, pp. 263–270, Anaheim, CA, Jan. 24-27, 1994.

[27] H. Seraji. Configuration control of redundant manipulators: Theory and implementation. *IEEE Trans. Robotics and Automation*, 5(4):472–490, Aug. 1989.

[28] D. Sreevijayan, S. Tosunoglu, and D. Tesar. Architectures for fault-tolerant mechanical systems. *Proc. 7th Mediterranean Electrotechnical Conf.*, pp. 1029–1033, Antalya, Turkey, Apr. 12-14, 1994.

[29] Y. Ting, S. Tosunoglu, and D. Tesar. A control structure for fault-tolerant operation of robotic manipulators. *IEEE Int. Conf. Robotics and Automation*, pp. 684–690, Atlanta, Georgia, May 2-6, 1993.

[30] M. L. Visinsky, J. R. Cavallaro, and I. D. Walker Robotic fault detection and fault tolerance: A survey. *Reliability Eng. System Safety*, 46:139–158, 1994.

[31] M. L. Visinsky, J. R. Cavallaro, and I. D. Walker. A dynamic fault tolerance framework for remote robots. *IEEE Trans. Robotics and Automation*, 11(4):477–490, Aug. 1995.

[32] E. C. Wu, J. C. Hwang, and J. T. Chladek. Fault-tolerant joint development for the space shuttle remote manipulator system: Analysis and experiment. *IEEE Trans. Robotics and Automation*, 9(5):675–684, Oct. 1993.

[33] T. Yoshikawa. Manipulability of robotic mechanisms. *Int. J. Robotics Res.*, 4(2):3–9, Summer 1985.